Inorg. Chem. **2004**, *43*, 7916–7925

Forum

Design, Folding, and Activities of Metal-Assembled Coiled Coil Proteins

Allison J. Doerr[†] and George L. McLendon*[,‡]

Departments of Chemistry, Princeton University, Princeton, New Jersey 08544, and Duke University, Durham, North Carolina 27708

Received July 16, 2004

Metal ions serve many purposes in natural proteins, from the stabilization of tertiary structure to the direction of protein folding to crucial roles in electron transfer and catalysis. There is considerable interest in creating metal binding sites in designed proteins to understand the structural role of metal ions and to design new metalloproteins with useful functions. The de novo design of metalloproteins and the role of metals in the folding of designed proteins are reviewed here, with particular focus on the design, folding, and activities of the $[M(bpy\text{-}peptide)_3]^{2+}$ structure. This maquette is constructed by the covalent attachment of 2,2′-bipyridine to the N-termini of amphiphilic peptides, and it is assembled into a folded trimeric coiled coil by the addition of a six-coordinate transition metal ion and the resulting hydrophobic collapse of the peptides. The $[M(bpy\text{-}peptide)_3]^{2+}$ structure has been employed in diverse applications, ranging from electron transfer pathway studies to the study of optimal hydrophobic packing in a virtual library to the construction of receptors and biosensors.

The Protein Folding Problem and de Novo Protein Design

Although great advances have been made, proteins continue to remain challenging targets for design. The difficulty lies in the notorious protein folding problem; that is, we do not fully understand the unique balance of forces that cause a linear primary polypeptide sequence to fold into a singular, functioning tertiary structure.[1] De novo protein design can help elucidate the rules and regulations governing protein folding by providing an arena to experimentally illuminate protein folding outcomes. Protein design also provides a means to create new proteins with unique catalytic or biosensing functions, performing processes unknown in nature. We will focus here not on the modification of natural proteins, but on the de novo design of truly novel protein structures.

Native structure in natural proteins is determined by a number of forces working in synergy to produce the lowest energy conformation. These stabilizing factors include the hydrophobic effect, van der Waals packing interactions, hydrogen bonding, electrostatic interactions, and disulfide bond formation.[2] Many designed proteins do not fold properly into one native folded structure but have compact yet flexible structures capable of fulfilling several low-energy conformations, such that secondary structure is well defined but tertiary structure may not be. These structures have been termed molten globules, and the state has been proposed as an intermediate stage in protein folding (Figure 1).[3] The destabilization of alternate conformations, known as negative design, can help to overcome this problem (such as by designing repulsive electrostatic interactions to prevent alternate folds).[4] However, we still do not understand enough about the energetics of protein folding in order to rationally design de novo proteins with nativelike structure. Furthermore, the larger the designed structure, the more uncertain the folding. For now, shortcuts must be made to circumvent the protein folding problem in order to design proteins with useful functions.

* Corresponding author. E-mail: george.mclendon@duke.edu.
[†] Princeton University.
[‡] Duke University.

(1) Yon, J. M. *Braz. J. Med. Biol. Res.* **2001**, *34*, 419−435.
(2) (a) Matthews, B. W. *Annu. Rev. Biochem.* **1993**, *62*, 139−160. (b) Dill, K. A. *Biochemistry* **1990**, *29*, 7133−7155. (c) Alber, T. *Annu. Rev. Biochem.* **1989**, *58*, 765−798.
(3) (a) Ohgushi, M.; Wada, A. *FEBS Lett.* **1983**, *164*, 21−24. (b) Ptitsyn, O. B.; Pain, R. H.; Semisotnov, G. V.; Zerovnik, E.; Razgulyaev, O. I. *FEBS Lett.* **1990**, *262*, 20−24. (c) Kaltashov, I. A.; Eyles, S. J. *Mass Spectrom. Rev.* **2002**, *21*, 37−71. (d) Dyson, H. J.; Wright, P. E. *Chem. Rev.* **2004**, *104*, 3607−3622.
(4) (a) Baltzer, L.; Nilsson, H.; Nilsson, J. *Chem. Rev.* **2001**, *101*, 3153−3163. (b) Kohn, W. D.; Hodges, R. S. *Trends Biotech.* **1998**, *16*, 379−389.

10.1021/ic0490573 CCC: $27.50
Published on Web 11/06/2004

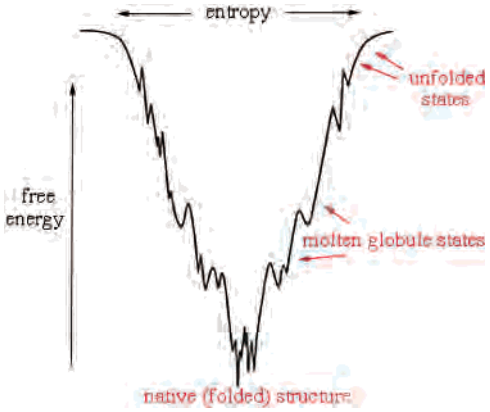

Figure 1. Cross-section of a protein folding landscape, depicted as a rugged funnel.[5] The native structure has the lowest energy. Unfolded states are high-energy, but there are many more conformations available. Molten globule states are relatively low-energy, but there still are several conformations available.

The Coiled Coil

Small model proteins are the simplest and most robust structures to design and construct. The coiled coil is a very common folding motif in nature, found in such diverse structures as cell "skeletal" proteins and motor proteins, yet also serving to mediate globular protein−protein interactions and DNA binding.[6] It is an extremely useful and versatile maquette for de novo protein design.[7] Short, prohelical peptides may easily be synthesized on a resin by standard methods of solid-phase peptide synthesis (SPPS).

A coiled coil consists of two to six amphiphilic α-helices that are wound into a left-handed superhelix, thus reducing the number of residues per turn to effectively 3.5 with respect to the superhelix axis (rather than 3.6 residues per turn as for an isolated α-helix). A binary pattern of hydrophobic and hydrophilic residues is necessary and sufficient for proper secondary structure folding.[8] The binary code for an α-helix is a heptad repeat of residues, labeled *a*−*g* (Figure 2). Side chains *a* and *d* are typically hydrophobic, as they mediate the hydrophobic collapse at the helix interface. Designed sequences often place bulky branched hydrophobic residues (such as valine, leucine, and isoleucine) in these positions to optimize van der Waals packing. Residues *b*, *c*, *e*, *f*, and *g* are usually hydrophilic, since they are exposed to solvent. Oppositely charged residues are often placed in positions *e* and *g* for increased stability, as they are complementary between helices.[9]

Like any protein structure, the hydrophobic effect is the driving force for folding of coiled coil domains. However, the number of helices in the coiled coil, or oligomeric state, is determined by more specific interactions. The van der Waals packing of the core can specify oligomeric state.[10] For example, a sequence with isoleucine in the *a* position

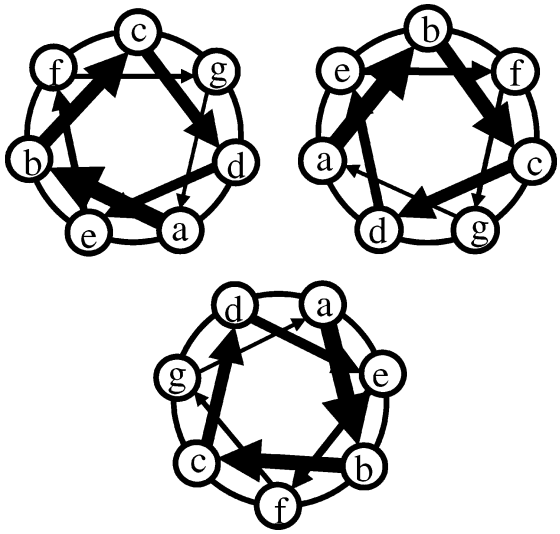

Figure 2. Trimeric helix wheel diagram, looking down at two turns of the helix (one heptad). Residues *a* and *d* are hydrophobic, *e* and *g* are often oppositely charged, and *b*, *c*, and *f* are hydrophilic.

and leucine in the *d* position (I*a*L*d*) formed dimers, I*a*I*d* formed trimers, and L*a*I*d* formed tetramers.[11] However, V*a*I*d*, V*a*L*d*, L*a*V*d*, and L*a*L*d* formed a mixture of oligomerization states. The steric matching of hydrophobic side chains can play a role in predetermining coiled coil topology but is not always sufficient for specificity. Loop regions designed by breaks in the helical heptad repeat can connect helical regions, thus specifying the topology of the bundle.[12] Polar residues in the core (in *a* or *d* positions) often specify a dimeric state due to the formation of complementary buried interhelical hydrogen bonds.[13] Disulfide bonds form interhelical cross-links to stabilize dimeric structures as well.[14] As we will see in the following sections, metals can also mediate coiled coil assembly and specify oligomeric state.

Metal Binding Sites in Designed Proteins

It is estimated that approximately one-third of all natural proteins contain metal ions.[15] Metals play crucial roles as cofactors in numerous proteins, serving in the stabilization

(5) Adapted from: Onuchic, J. N.; Luthey-Schulten, Z.; Wolynes, P. G. *Annu. Rev. Phys. Chem.* **1997**, *48*, 545−600.
(6) (a) Burkhard, P.; Stetefeld, J.; Strelkov, S. V. *Trends Cell Biol.* **2001**, *11*, 82−88. (b) Lupas, A. *Trends Biochem. Sci.* **1996**, *21*, 375−382.
(7) Mason, J. M.; Arndt, K. M. *ChemBioChem* **2004**, *5*, 170−176.
(8) (a) Kamtekar, S.; Schiffer, J. M.; Xiong, H.; Babik, J. M.; Hecht, M. H. *Science* **1993**, *262*, 1680−1685. (b) Moffet, D. A.; Hecht, M. H. *Chem. Rev.* **2001**, *101*, 3191−3203. (c) Hecht, M. H.; Das, A.; Go, A.; Bradley, L. H.; Wei, Y. *Protein Sci.* **2004**, *13*, 1711−1723.
(9) (a) Kohn, W. D.; Kay, C. M.; Hodges, R. S. *J. Mol. Biol.* **1998**, *283*, 993−1012. (b) Kohn, W. D.; Kay, C. M.; Hodges, R. S. *Protein Sci.* **1995**, *4*, 237−250.
(10) (a) Nautiyal, S.; Woolfson, D. N.; King, D. S.; Alber, T. *Biochemistry* **1995**, *34*, 11645−11651. (b) Boice, J. A.; Dieckmann, G. R.; DeGrado, W. F.; Fairman, R. *Biochemistry* **1996**, *35*, 14480−14485. (c) Suzuki, K.; Hiroaki, H.; Kohda, D.; Tanaka, T. *Protein Eng.* **1998**, *11*, 1051−1055. (d) Kashiwada, A.; Hiroaki, H.; Kohda, D.; Nango, M.; Tanaka, T. *J. Am. Chem. Soc.* **2000**, *122*, 212−215. (e) Schnarr, N. A.; Kennan, A. J. *J. Am. Chem. Soc.* **2001**, *123*, 11081−11082.
(11) Harbury, P. B.; Zhang, T.; Kim, P. S.; Alber, T. *Science* **1993**, *262*, 1401−1407.
(12) (a) Hill, R. B.; Raleigh, D. P.; Lombardi, A.; DeGrado, W. F. *Acc. Chem. Res.* **2000**, *33*, 745−754. (b) DeGrado, W. F.; Summa, C. M.; Pavone, V.; Nastri, F.; Lombardi, A. *Annu. Rev. Biochem.* **1999**, *68*, 779−819. (c) Venkatraman, J.; Shankaramma, S. C.; Balaram, P. *Chem. Rev.* **2001**, *101*, 3131−3152.
(13) (a) O'Shea, E. K.; Klemm, J. D.; Kim, P. S.; Alber, T. *Science* **1991**, *254*, 539−544. (b) Gonzalez, L., Jr.; Woolfson, D. N.; Alber, T. *Nat. Struct. Biol.* **1996**, *3*, 1011−1018. (c) Akey, D. L.; Malashkevich, V. N.; Kim, P. S. *Biochemistry* **2001**, *40*, 6352−6360. (d) Campbell, K. M.; Sholders, A. J.; Lumb, K. J. *Biochemistry* **2002**, *41*, 4866−4871.
(14) (a) Kuroda, Y. *Protein Eng.* **1995**, *8*, 97−101. (b) Zhou, N. E.; Kay, C. M.; Hodges, R. S. *Biochemistry* **1993**, *32*, 3178−3187.
(15) Holm, R. H.; Kennepohl, P.; Solomon, E. I. *Chem. Rev.* **1996**, *96*, 2239−2314.

of structure, electron transfer, ligand binding and transport, and catalysis. In this section, we will focus on the structural role metal ions provide to designed proteins.

From a practical standpoint, the detection of metal ions in proteins is relatively easy compared to the determination of protein structure (by crystallography or NMR). Optical spectroscopy, NMR, and EPR may be used to characterize metal binding sites, and consequently, one may learn quite a bit about the protein in question without solving a full three-dimensional crystal structure.[16]

Metal binding sites in proteins are often classified under one of two categories. One type is a preorganized metal binding site, such that metal binding only occurs if the protein ligands are in the correct conformation. Preorganized sites often have unusual geometries at the metal center, which can result in an enhanced propensity for electron transfer or catalysis. Blue copper proteins are good examples of this category; they are completely folded in the absence of metal ion. Moreover, blue copper sites have strong redox activity due to the ligand-imposed distorted tetrahedral geometry at the metal center.[17]

In the other type of metal binding site, protein folding is metal-directed; the binding site is not preorganized. In fact, the protein may be quite unstructured in the absence of the metal ion. The metal usually has a solely structural responsibility in these types of sites; it is responsible for protein folding and stabilization but rarely plays a catalytic role. Zinc finger proteins are an example of this type of metal binding site; they are completely unfolded in the absence of metal ion.[18] They serve in nature as DNA-binding gene regulatory proteins. These two examples demonstrate the extremes of metal−protein interactions; in reality, most metal binding sites fall somewhere on a continuum between blue copper and zinc finger proteins.

Early work in the design of metal binding sites showed that protein secondary structure could be stabilized by metal ions. For example, Ghadiri and co-workers stabilized α-helical structure in short peptides using metal ions.[19] Peptides with amphiphilic sequences of less than about 20 amino acids are not typically helical in aqueous solution, due to the large energetic price to pay for the nucleation of the first turn. The overall energy gained by folding is not sufficient to initiate this first nucleation step. However, when either cysteine or histidine residues were placed in positions $i + 4$ and i (one turn apart), these side chains ligated a transition metal ion which forced the formation of this first turn, and subsequently nucleated the α-helix. The metal ion acted as a cross-linking agent to stabilize the fold by diminishing the entropy of the unfolded state relative to the folded state. A similarly designed random coil peptide as short as 11 residues was reported to be converted to an α-helix by the addition of a transition metal.[20] This idea has also been employed in the design of a high-throughput screen to scan a combinatorial peptide library for folded dimeric coiled coils by immobilized metal-affinity chromatography (IMAC).[21] When a particular dimer was folded, histidines in positions $i + 4$ and i ligated the immobilized metal (in this case, a nickel(II)-charged imino diacetate column). The poorly folded peptides without a well-defined metal binding site were washed away, and then the properly folded peptides fixed to the column were eluted and identified.

Many groups have been successful in stabilizing the tertiary fold of designed proteins by the insertion of metal binding sites. The DeGrado group designed a four-helix bundle protein, α4, where the helices were connected by loops.[22] While this protein was globally quite stable, it exhibited many characteristics of a molten globule, such as poor dispersion in the ^{1}H NMR spectrum, binding of the hydrophobic dye 1-anilino-8-naphthalene sulfonate (ANS), and a noncooperative thermal transition. However, by designing in a metal binding site, the protein exhibited much more nativelike behavior due to the specificity of metal ligation conferring a unique structure.[23] The Regan group discovered a similar result in a designed four-helix bundle protein with an introduced tetrahedral zinc(II) binding site.[24]

Metal ion ligation has also been used to define tertiary folds by joining secondary structural elements. The Hodges group designed a dimeric coiled coil protein that was destabilized in the absence of metal, due to electronic repulsions of either glutamic acid (Glu) or γ-carboxyglutamic acid (Gla) side chains at both positions e and g.[25] When lanthanum was added (in the form of $LaCl_3$), it coordinated the two Glu or Gla side chains on either side of the helix bundle, effectively bridging the two residues and stabilizing the dimer. The Pecoraro group designed trimeric coiled coils with buried cysteine residues that were stabilized upon the binding of mercury(II),[26] arsenic(III),[27] or cadmium(II).[28] The Tanaka group introduced six histidine ligands into the core

(16) Regan, L. *Annu. Rev. Biophys. Biomol. Struct.* **1993**, *22*, 257−281.
(17) (a) Solomon, E. I.; Szilagyi, R. K.; DeBeer, G. S.; Basumallick, L. *Chem. Rev.* **2004**, *104*, 419−458. (b) Gray, H. B.; Malmstrom, B. G.; Williams, R. J. P. *J. Biol. Inorg. Chem.* **2000**, *5*, 551−559. (c) Hellinga, H. W. *J. Am. Chem. Soc.* **1998**, *120*, 10055−10066. (d) Schnepf, R.; Horth, P.; Bill, E.; Wieghardt, K.; Hildebrandt, P.; Haehnel, W. *J. Am. Chem. Soc.* **2001**, *123*, 2186−2195.
(18) (a) Berg, J. M.; Godwin, H. A. *Annu. Rev. Biophys. Biomol. Struct.* **1997**, *26*, 357−371. (b) Cox, E. H.; McLendon, G. L. *Curr. Opin. Chem. Biol.* **2000**, *4*, 162−165.
(19) (a) Ghadiri, M. R.; Choi, C. *J. Am. Chem. Soc.* **1990**, *112*, 1630−1632. (b) Ghadiri, M. R.; Fernholz, A. K. *J. Am. Chem. Soc.* **1990**, *112*, 9633−9635.
(20) Ruan, F.; Chen, Y.; Hopkins, P. B. *J. Am. Chem. Soc.* **1990**, *112*, 9403−9404.
(21) Fujii, I.; Takaoka, Y.; Suzuki, K.; Tanaka, T. *Tetrahedron Lett.* **2001**, *42*, 3323−3325.
(22) Regan, L.; DeGrado, W. F. *Science* **1988**, *241*, 976−978.
(23) (a) Handel, T.; DeGrado, W. F. *J. Am. Chem. Soc.* **1990**, *112*, 6710−6711. (b) Handel, T. M.; Williams, S. A.; DeGrado, W. F. *Science* **1993**, *261*, 879−885.
(24) Regan, L.; Clarke, N. D. *Biochemistry* **1990**, *29*, 10878−10883.
(25) (a) Kohn, W. D.; Kay, C. M.; Hodges, R. S. *J. Pept. Res.* **1998**, *51*, 9−18. (b) Kohn, W. D.; Kay, C. M.; Sykes, B. D.; Hodges, R. S. *J. Am. Chem. Soc.* **1998**, *120*, 1124−1132.
(26) (a) Dieckmann, G. R.; McRorie, D. K.; Tierney, D. L.; Utschig, L. M.; Singer, C. P.; O'Halloran, T. V.; Penner-Hahn, J. E.; DeGrado, W. F.; Pecoraro, V. L. *J. Am. Chem. Soc.* **1997**, *119*, 6195−6196. (b) Farrer, B. T.; Harris, N. P.; Balchus, K. E.; Pecoraro, V. L. *Biochemistry* **2001**, *40*, 14696−14705.
(27) Farrer, B. T.; McClure, C. P.; Penner-Hahn, J. E.; Pecoraro, V. L. *Inorg. Chem.* **2000**, *39*, 5422−5423.
(28) Matzapetakis, M.; Farrer, B. T.; Weng, T.-C.; Hemmingsen, L.; Penner-Hahn, J. E.; Pecoraro, V. L. *J. Am. Chem. Soc.* **2002**, *124*, 8042−8054.

of a putative trimeric coiled coil.[29] In the absence of a metal, the coiled coil was destabilized due to the unfavorable hydrophobic burial of six polar histidines. However, when a transition metal such as nickel(II), cobalt(II), or zinc(II) was introduced, a stable trimer formed.

The Imperiali group incorporated un-natural amino acid side chains with metal-chelating groups into a β-hairpin motif.[30] The bidentate ligands 2,2′-bipyridine and 1,10-phenanthroline are excellent coordinating agents due to the chelate effect and their π-accepting abilities. These ligands were incorporated into the protein as un-natural amino acids, and their metal binding affinities were found to be much higher than natural metal ligating amino acids. As we shall see, this provides a good transition to understanding the metal binding sites employed in our laboratory.

Templates, Protein Folding, and the $[M(bpy\text{-}peptide)_3]^{2+}$ Maquette

As described earlier, the design of a protein sequence that will fold into a topologically predetermined structure is not an easy task, given that the rules that govern protein folding have not been fully elucidated. However, the protein designer has tools available that nature does not possess that allow us to make shortcuts. By anchoring amphiphilic secondary structure elements to a rigid template in a branched arrangement, tertiary protein structure may be topologically predetermined. The concept of template-assembled synthetic proteins, or TASP, was first introduced by Mutter and co-workers.[31]

The TASP approach assembles secondary structural blocks in close proximity, thus decreasing the substantial energy barriers that exist for the folding of random coil sequences. In addition, because of the reduced conformational space accessible to TASP structures, they show a higher thermodynamic stability than their unbranched analogues. The short-range interactions induced by the template promote proper folding and discourage intermolecular aggregation. The oligomeric state of the structure is unambiguous because the peptides are fixed to the rigid template. TASP template molecules include β-hairpin oligopeptides,[31] cyclic peptides,[32] and organic molecules.[33] In addition, they are promising maquettes for the development of biosensors.[34]

A metal binding site can also be thought of as a template for protein folding; this idea was independently developed by Ghadiri and co-workers[35] and Sasaki and co-workers.[36] A 2,2′-bipyridine ligand (bpy) was covalently appended to the N-terminus of an amphiphilic peptide designed by binary patterning. 2,2′-Bipyridine ligands are desirable for many reasons: they react readily with a variety of metals and are well-studied inorganic complexes, they have high thermodynamic and kinetic stabilities, and they serve as excellent spectroscopic probes. When a six-coordinate transition metal ion such as iron(II), cobalt(II), or nickel(II) was introduced, an octahedral complex formed with three bidentate bipyridine ligands donating to the metal ion. Thus, a rigid molecule served as a template to assemble tertiary coiled coil structure, but the physical association was controlled by metal binding.

Because the peptides were designed as amphiphilic α-helical sequences, the main driving force for folding was the hydrophobic effect, but the metal ion specified the oligomeric state of the coiled coil as unambiguously trimeric. These peptides were also quite short, so as to be relatively unstructured without the presence of the metal ion. As the metal ion forced the peptides into proximity, by burial of the hydrophobic residues they formed stable α-helices (Figure 3).[37] Both groups noted a significant increase in helicity by circular dichroism with the addition of the metal ion. As we shall see, this $[M(bpy\text{-}peptide)_3]^{2+}$ maquette can be utilized in various applications.

A closer look at this maquette confirmed that metal binding and protein folding were tightly coupled.[38] A 20-residue peptide P_{20} was designed with leucines in positions *a* and *d*, to favor a dimer or antiparallel coiled coil arrangement rather than a parallel trimer.[39] This was purposeful, ensuring that the trimer was destabilized in the absence of a metal in order to study the role of the metal as a promoter of trimeric structure. Helicity increased from about 66% in the absence of a metal to greater than 87% in the presence of either Ni(II) or Co(II).

Because of the amino acid sequence degeneracy of P_{20}, it was difficult to assign and interpret multidimensional ^{1}H NMR spectra.[38] However, Ni(II) and Co(II) are paramagnetic metal ions. When either metal was present in the structure, the degeneracy was lifted because pseudocontact NMR shifts are dependent on the distance from the paramagnetic center; thus, the same amino acid at different locations in the sequence will have different chemical shifts. The folding of P_{20} was compared to P_3, a peptide of only three amino acids with essentially no tertiary structure. It was found that the C-terminal end of P_{20} was well-folded, but the bipyridine-modified N-terminus was poorly folded. Co(II) exchanged 10 times as fast out of the P_{20} as the P_3 complex, perhaps

(29) (a) Suzuki, K.; Hiroaki, H.; Kohda, D.; Nakamura, H.; Tanaka, T. *J. Am. Chem. Soc.* **1998**, *120*, 13008−13015. (b) Kiyokawa, T.; Kanaori, K.; Tajima, K.; Tanaka, T. *Biopolymers* **2000**, *55*, 407−414.
(30) Cheng, R. P.; Fisher, S. L.; Imperiali, B. *J. Am. Chem. Soc.* **1996**, *118*, 11349−11356.
(31) (a) Mutter, M.; Tuchscherer, G. *Makromol. Chem., Rapid Commun.* **1988**, *9*, 437−443. (b) Mutter, M.; Vuilleumier, S. *Angew. Chem., Int. Ed. Engl.* **1989**, *28*, 535−554. (c) Tuchscherer, G.; Mutter, M. *J. Biotech.* **1995**, *41*, 197−210.
(32) (a) Mutter, M.; Tuchscherer, G. G.; Miller, C.; Altmann, K.-H.; Carey, R. I.; Wyss, D. F.; Labhardt, A. M.; Rivier, J. E. *J. Am. Chem. Soc.* **1992**, *114*, 1463−1470. (b) Tuchscherer, G.; Grell, D.; Mathieu, M.; Mutter, M. *J. Peptide Res.* **1999**, *54*, 185−194.
(33) (a) Goodman, M.; Feng, Y.; Melacini, G.; Taulane, J. P. *J. Am. Chem. Soc.* **1996**, *118*, 5156−5157. (b) Gibb, B. C.; Mezo, A. R.; Sherman, J. C. *Tetrahedron Lett.* **1995**, *36*, 7587−7590. (c) Causton, A. S.; Sherman, J. C. *Bioorg. Med. Chem.* **1999**, *7*, 23−27.
(34) (a) Tuchscherer, G.; Scheibler, L.; Dumy, P.; Mutter, M. *Biopolymers* **1998**, *47*, 63−73. (b) Scheibler, L.; Dumy, P.; Stamou, D.; Duschl, C.; Vogel, H.; Mutter, M. *Polym. Bull.* **1998**, *40*, 151−157.
(35) Ghadiri, M. R.; Soares, C.; Choi, C. *J. Am. Chem. Soc.* **1992**, *114*, 825−831.
(36) Lieberman, M.; Sasaki, T. *J. Am. Chem. Soc.* **1991**, *113*, 1470−1471.
(37) Case, M. A.; McLendon, G. L. *Acc. Chem. Res.* **2004**, *37*, 754−762.
(38) Gochin, M.; Khorosheva, V.; Case, M. A. *J. Am. Chem. Soc.* **2002**, *124*, 11018−11028.
(39) (a) Lovejoy, B.; Choe, S.; Cascio, D.; McRorie, D. K.; DeGrado, W. F.; Eisenberg, D. *Science* **1993**, *259*, 1288−1293. (b) Bryson, J. W.; Desjarlais, J. R.; Handel, T. M.; DeGrado, W. F. *Protein Sci.* **1998**, *7*, 1404−1414.

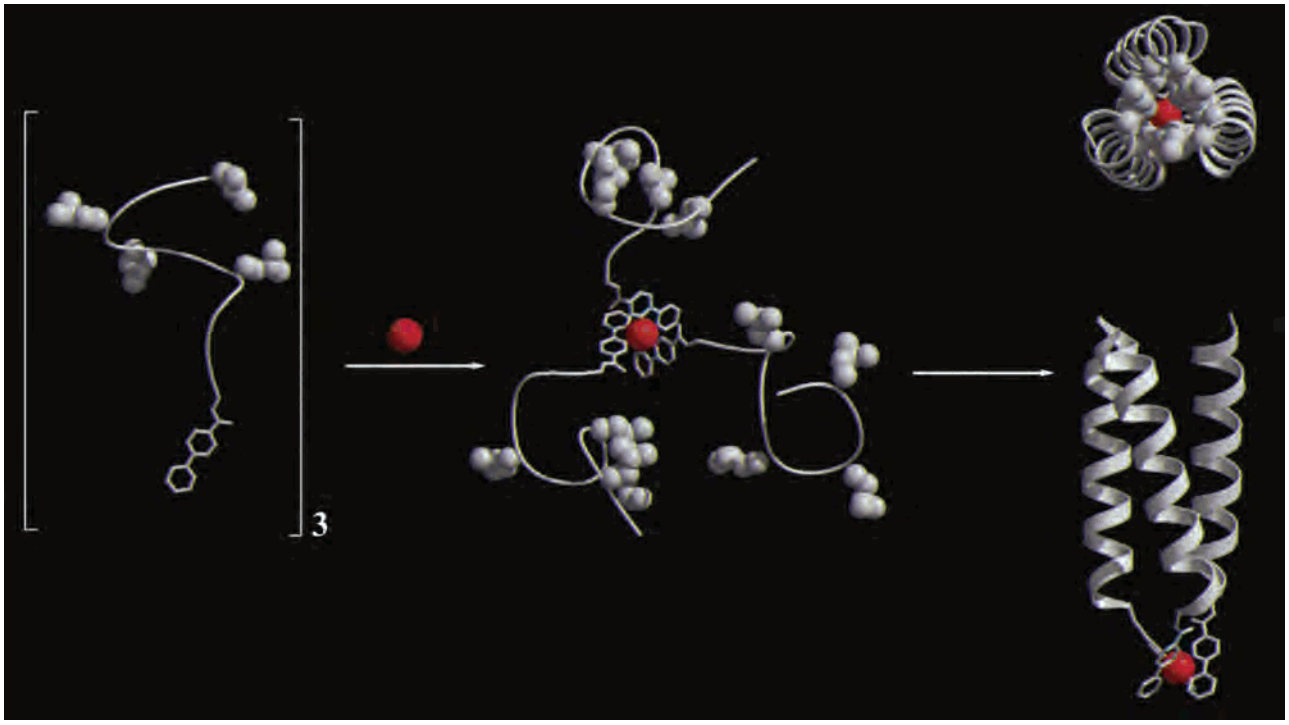

Figure 3. Proposed model for metal assembly of the trimeric coiled coil $[M(bpy\text{-}peptide)_3]^{2+}$.[37] A six-coordinate metal ion tethers three 2,2′-bipyridine ligands covalently connected to amphiphilic peptides (left), which undergo hydrophobic collapse to yield the folded structure (right).

owing to the distortion of the octahedral tris-bipyridine geometry resulting from the hydrophobic collapse of the peptides. In addition, P_3 was likely to form significant amounts of dimer with Co(II), whereas P_{20} formed only trimers, indicating that protein folding greatly influenced the third bipyridine binding constant, since K_2 is greater than K_3 for $[Co(bpy)_3]^{2+}$ complexes.

The chemoselectivity of metal−ligand complexes has also been employed to construct four-helix and two-helix bundles. A parallel four-helix bundle was created by covalently attaching a modified pyridine (pyr) ligand to the N-terminus of an amphiphilic peptide.[40] Upon addition of a $Ru_5Cl_{12}^{2-}$ cluster, the $[Ru(pyr\text{-}peptide)_4Cl_2]$ complex formed. The design of stable metal-assembled dimers was accomplished by synthesizing and covalently attaching terpyridines (terpy) to the N-terminus of peptides, forming the octahedral $[Fe(terpy\text{-}peptide)_2]^{2+}$ complex upon addition of iron(II).[41]

Applications and Activities of Metal-Assembled Proteins

One goal of protein design is to create proteins with useful functions, and the McLendon group has made significant contributions in that arena. We have employed this metal-assembled trimeric coiled coil construct in diverse applications, ranging from the design of electron transfer proteins, to the study of packing and stereoselection in virtual combinatorial libraries, to the design of receptors and biosensors.

Designed Coiled Coil Proteins for Electron Transfer Studies

Electron transfer (ET) reactions are crucial in many natural energy transfer processes, from photosynthesis to respiration to the nitrogen cycle, most of which are mediated by proteins. The mechanism of electron transfer has been thoroughly explored in natural proteins.[42] However, designed synthetic proteins provide a testing ground for electron transfer theory, especially in offering a relatively simple means for backbone structural modification.

The simplest model for electron transfer states that the rate of electron transfer is exponentially correlated to distance[43]

$$k_{ET} \propto \exp(-\beta R)$$

where k_{ET} is the electron transfer rate constant, β is the electronic damping factor (decay constant), and R is the distance between the electron donor and acceptor. However, electron transfer is much more efficient when the electron travels through bonds rather than through space. In proteins, especially in α-helices, the covalent pathway could be quite long compared to the through-space distance, so the electron may compromise by tunneling through a combination of covalent bonds, hydrogen bonds, and other nonbonded interactions.[44] There is some debate as to whether electron transfer occurs through one dominant "best" pathway of bonds, or if there are multiple pathways available through

(40) Ghadiri, M. R.; Soares, C.; Choi, C. *J. Am. Chem. Soc.* **1992**, *114*, 4000−4002.
(41) Vandermeulen, G. W. M.; Tziatzios, C.; Schubert, D.; Andres, P. R.; Alexeev, A.; Schubert, U. S.; Klok, H.-A. *Aust. J. Chem.* **2004**, *57*, 33−39.
(42) (a) Gray, H. B.; Winkler, J. R. *Annu. Rev. Biochem.* **1996**, *65*, 537−561. (b) Beratan, D. N.; Skourtis, S. S. *Curr. Opin. Chem. Biol.* **1998**, *2*, 235−243. (c) Larsson, S. *Biochim. Biophys. Acta* **1998**, *1365*, 294−300.
(43) Marcus, R. A.; Sutin, N. *Biochim. Biophys. Acta* **1985**, *811*, 265−322.

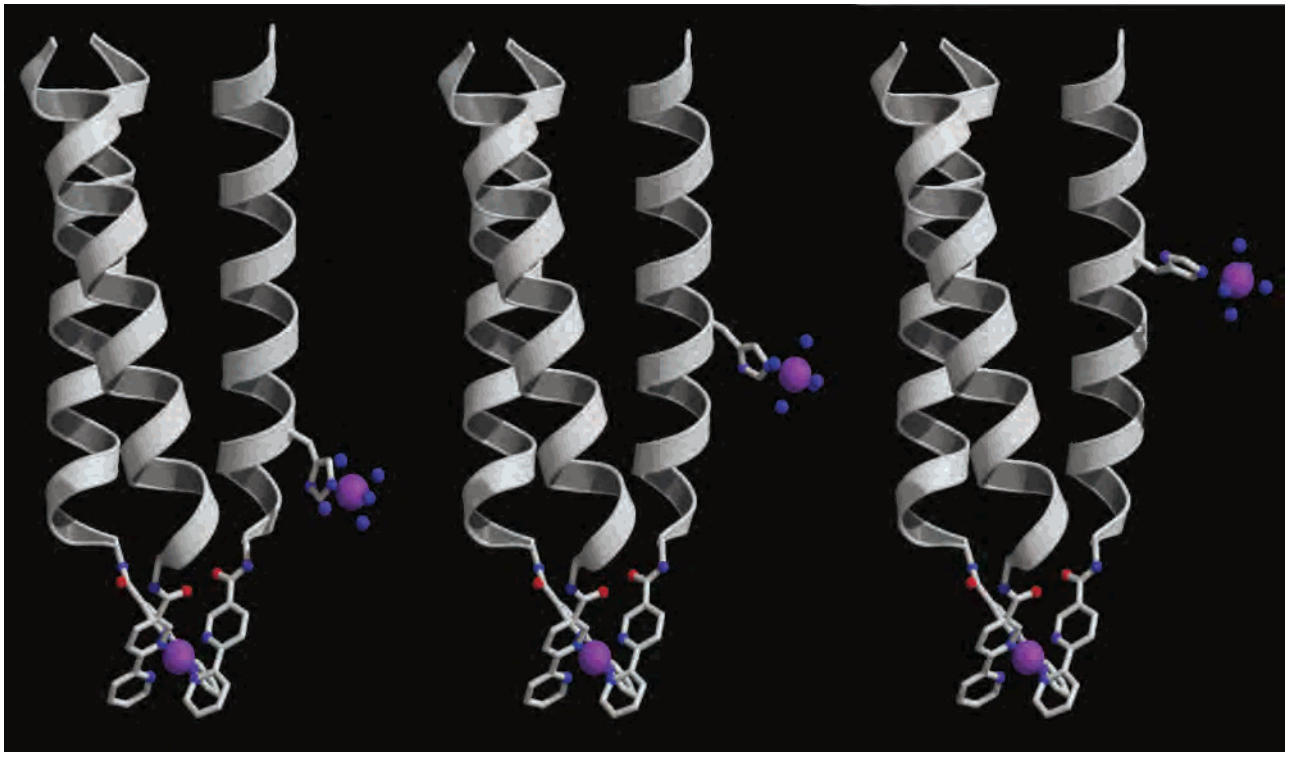

Figure 4. Models of three variants of the Ru(III)(His)$(NH_3)_5$ electron transfer protein, with the electron acceptor shown one turn (left, 15 Å ET distance, 1×10^6 s^{-1} ET rate), two turns (center, 20 Å, 1×10^4 s^{-1}), and three turns (right, 25 Å, 1×10^2 s^{-1}) from the $[Ru(bpy)_3]^{2+}$ electron donor moiety.[37,47]

the "averaged" intervening medium (an extension of the pure distance model).[45] These questions were investigated by the McLendon group using the $[M(bpy\text{-}peptide)_3]^{2+}$ coiled coil construct.

Well-folded proteins with backbone hydrogen bonds intact are expected to be more efficient electron shuttles than poorly folded proteins, so the role of helical secondary structure in controlling electron transfer was explored in the first reported designed electron transfer protein.[46] $[Co(bpy)_3]^{3+}$ served as the electron acceptor at the N-terminus of the coiled coil. The donor, at the C-terminus of the 16-residue peptides, was 1-ethyl-1′-ethyl-4,4′-bipyridinium. Electron transfer rates were measured in denaturing conditions (6 M urea, 0% helicity) and helix-promoting conditions (25% trifluoroethanol, ≥75% helicity). There was a corresponding increase in the rate of electron transfer with increase of the helicity of the trimer, indicating that the electron path was not solely through covalent bonds.

Ruthenium(II) may be excited by laser light or an electron beam to donate an electron. To further explore the electron transfer properties of this protein maquette, histidine residues were introduced at solvent-exposed positions of one helix of the trimer, one, two, or three turns away from the $[Ru(bpy)_3]^{2+}$ moiety (Figure 4).[47] These histidines provided a binding site for the electron acceptor Ru(III)$(NH_3)_5$. The distance between the metal centers was predicted by modeling. The measured electron transfer rates were found to be consistent with the distance model of electron transfer theory, demonstrating that a protein could be designed with predictable electron transfer properties.

We also explored the question of one dominant electron transfer pathway versus multiple tunneling pathways. In the dominant pathway model, a hydrogen bond is determined to be worth about two covalent bonds in terms of the rate of electron transfer.[48] Removal of a backbone hydrogen bond is very difficult to engineer in a natural protein,[49] but it may be accomplished in a relatively straightforward fashion by solid-phase peptide synthesis and/or native chemical ligation.[50] A single backbone hydrogen bond proposed to lie on the dominant pathway was removed by replacing one amide bond with an ester bond, effectively deleting the hydrogen bond between the amide proton at position $i + 4$ with the carbonyl oxygen at position i.[51]

(44) (a) Beratan, D. N.; Onuchic, J. N.; Hopfield, J. J. *J. Chem. Phys.* **1987**, *86*, 4488−4498. (b) Beratan, D. N.; Betts, J. N.; Onuchic, J. N. *Science* **1991**, *252*, 1285−1288. (c) Wuttke, D. S.; Bjerrum, M. J.; Winkler, J. R.; Gray, H. B. *Science* **1992**, *256*, 1007−1009. (d) Beratan, D. N.; Onuchic, J. N.; Winkler, J. R.; Gray, H. B. *Science* **1992**, *258*, 1740−1741. (e) Winkler, J. R.; Gray, H. B. *J. Biol. Inorg. Chem.* **1997**, *2*, 399−404.

(45) (a) Regan, J. J.; Risser, S. M.; Beratan, D. N.; Onuchic, J. N. *J. Phys. Chem.* **1993**, *97*, 13083−13088. (b) Williams, R. J. P. *J. Biol. Inorg. Chem.* **1997**, *2*, 373−377. (c) Page, C. C.; Moser, C. C.; Chen, X.; Dutton, P. L. *Nature* **1999**, *402*, 47−52. (d) Jones, M. L.; Kurnikov, I. V.; Beratan, D. N. *J. Phys. Chem. A* **2002**, *106*, 2002−2006.

(46) Mutz, M. W.; McLendon, G. L.; Wishart, J. F.; Gaillard, E. R.; Corin, A. F. *Proc. Natl. Acad. Sci. U.S.A.* **1996**, *93*, 9521−9526.

(47) Mutz, M. W.; Case, M. A.; Wishart, J. F.; Ghadiri, M. R.; McLendon, G. L. *J. Am. Chem. Soc.* **1999**, *121*, 858−859.

(48) Onuchic, J. N.; Beratan, D. N. *J. Chem. Phys.* **1990**, *92*, 722−733.

(49) (a) Ellman, J. A.; Mendel, D.; Anthony-Cahill, S. J.; Noren, C. J.; Schultz, P. G. *Methods Enzymol.* **1991**, *202*, 301−336. (b) Chapman, E.; Thorson, J. S.; Schultz, P. G. *J. Am. Chem. Soc.* **1997**, *119*, 7151−7152. (c) Koh, J. T.; Cornish, V. W.; Schultz, P. G. *Biochemistry* **1997**, *36*, 11314−11322.

(50) (a) Kent, S. *J. Pept. Sci.* **2003**, *9*, 574−593. (b) Lu, W.; Qasim, M. A.; Laskowski, M., Jr.; Kent, S. B. H. *Biochemistry* **1997**, *36*, 673−679. (c) Low, D. W.; Hill, M. G. *J. Am. Chem. Soc.* **2000**, *122*, 11039−11040.

It was found by circular dichroism experiments that this hydrogen bond deletion did not significantly affect the helicity of the trimer. However, by guanidine hydrochloride denaturation, the hydrogen bond deletion was determined to cause a thermodynamic loss of about 0.7 kcal/mol. To investigate the effect on the rate of electron transfer, a histidine residue was placed two turns away from the $[Ru(bpy)_3]^{2+}$ moiety which, as described above, bound the electron acceptor $Ru(III)(NH_3)_5$. The deleted hydrogen bond was thus located on the same helix as and situated between the electron donor and acceptor. It was hypothesized that structural disruptions would have a significant impact on the rate of electron transfer, should the deletion lie on the dominant pathway. However, the results suggested only a very modest change in the ET rate from that of the hydrogen bond intact structure, which led to the conclusion that either this particular hydrogen bond did not lie on the dominant electron transfer pathway or that a dominant pathway did not exist.

In order to further explore this result, three variants were synthesized with the deleted hydrogen bond placed at three different positions on the helix: immediately adjacent to the Ru(III) redox site, one residue away, and two residues away.[52] It was predicted for a multiple pathway model of electron transfer that all peptides would react at the same rate, no matter the state of the hydrogen bond network, whereas a trend in reactivity was forecast from dominant pathway models. Again, the rates of electron transfer were comparable for all of the hydrogen bond deleted structures and the hydrogen bond intact structure. The results of this experiment showed that the electron transfer rate did not depend on a specific hydrogen bond pathway, thus further adding support to the theory of multiple electron transfer pathways in well-packed structures.

Packing Interactions and Metal Ligation

The $[M(bpy\text{-}peptide)_3]^{2+}$ maquette is a very useful construct to study the effects of metal ion binding and protein folding. Because metal ion binding and protein folding are coupled in this system, it can serve as a probe where the metal ligation effectively screens for the optimal packing interactions.

One of the consequences for a protein assembled by metal ligation is the formation of several isomers due to the geometry of the metal complex. For a six-coordinate octahedral metal complex composed of three unsymmetrical bidentate ligands, there are four possible diastereomers. There is the centrosymmetrical facial (*fac*) isomer and the asymmetrical meridional (*mer*) isomer, each of which can further be characterized as Λ or Δ enantiomers, such that the four structures are Λ-*fac*, Δ-*fac*, Λ-*mer*, and Δ-*mer* (Figure 5).

$[Ru(bpy)_3]^{2+}$ complexes are formed under kinetic control and are inert to ligand exchange. They assemble in the statistically expected ratio of 3:3:1:1 Λ-*mer*/Δ-*mer*/Λ-*fac*/Δ-*fac*. On the other hand, $[Fe(bpy)_3]^{2+}$ and other first-row transition metal complexes with bipyridine are formed under thermodynamic control and are exchange-labile, meaning that they can explore all possible geometries at the metal center until the lowest energy conformation is achieved. When peptides with a strong propensity for hydrophobic collapse are attached to the $[M(bpy)_3]^{2+}$ maquette, they can exert considerable stereochemical control over the metal ion ligation.

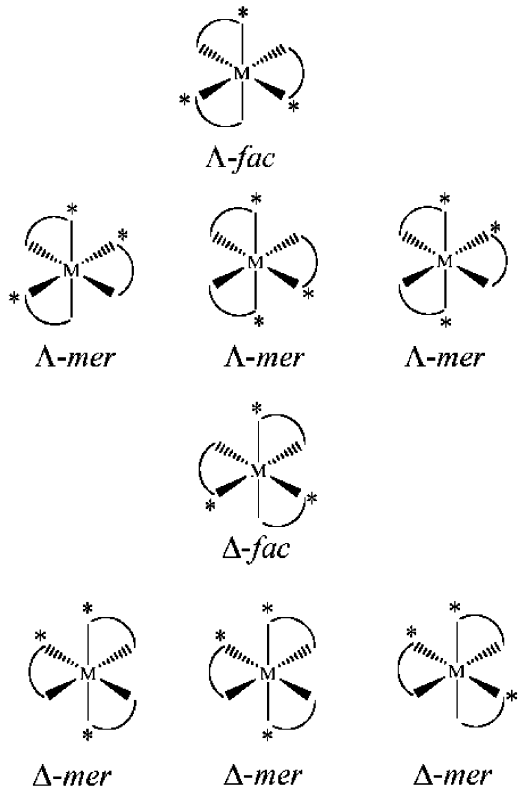

Figure 5. Possible stereochemical outcomes of $[M(bpy\text{-}peptide)_3]^{2+}$ complex formation. Bidentate 2,2′-bipyridine is indicated by an arc, and the peptide is indicated by an asterisk. Note that there are three possible *mer* arrangements for either the Λ or Δ enantiomer, leading to the statistically expected ratio of 3:3:1:1 Λ-*mer*/Δ-*mer*/Λ-*fac*/Δ-*fac*.

In earlier work by Sasaki and co-workers, it was found that, without optimized packing interactions, an iron(II)-assembled 15-residue peptide trimer formed nearly the expected ratio of isomers.[53] McLendon and co-workers made a similar study using both the exchange-inert ruthenium(II) and the exchange-labile iron(II) to investigate the stereoselection by a well-packed 20-residue peptide (P_{20}) coiled coil versus a 3-residue peptide (P_3) trimer with essentially no tertiary structure.[54] It was found that $[Ru(P_3)_3]^{2+}$ formed isomers with the statistically expected ratio described above. However, $[Ru(P_{20})_3]^{2+}$ assembled as an 80% excess of *fac* isomer. With iron(II), the effect was even more pronounced: essentially all $[Fe(P_{20})_3]^{2+}$ assembled as the *fac* isomer. Furthermore, it could be deduced by circular dichroism that the Λ-*fac* isomer formed in 40% excess over the

(51) Zhou, J.; Case, M. A.; Wishart, J. F.; McLendon, G. L. *J. Phys. Chem. B* **1998**, *102*, 9975−9980.
(52) Zheng, Y.; Case, M. A.; Wishart, J. F.; McLendon, G. L. *J. Phys. Chem. B* **2003**, *107*, 7288−7292.
(53) (a) Lieberman, M.; Tabet, M.; Sasaki, T. *J. Am. Chem. Soc.* **1994**, *116*, 5035−5044. (b) Sasaki, T.; Lieberman, M. *Tetrahedron* **1993**, *49*, 3677−3689.
(54) Case, M. A.; Ghadiri, M. R.; Mutz, M. W.; McLendon, G. L. *Chirality* **1998**, *10*, 35−40.

Δ-*fac* isomer, which was attributed to more favorable interhelical packing interactions in the Λ conformation.

To further explore packing interactions in a trimeric, metal-assembled protein maquette, the self-assembly process and the lability of iron(II) were exploited to create a virtual combinatorial library.[55] Combinatorial experiments are useful when screening for an optimal property, such as the most favorable packing in a coiled coil construct. However, in a synthesis-directed combinatorial library, all possible sequences must be synthesized and screened, which can be difficult and time-consuming. A virtual library takes advantage of the self-assembly process to employ it as a self-screening process through equilibration based on noncovalent interactions, greatly simplifying the detection and identification of the "winners".[56]

Three peptides, αpA, αpL, and αpLA, were synthesized, and bipyridine was covalently attached.[55] The peptides were allowed to self-assemble with a substoichiometric quantity of iron(II), such that only the most stable trimers formed. Iron(II) was chosen because of its lability and extremely large third bipyridine binding constant, which ensures trimer formation. By size exclusion chromatography, trimers were separated from the monomers. The peptides were also assembled in all possible combinations as 11 exchange-inert ruthenium(II) complexes, and the unfolding free energies ($\Delta G_u°$) were determined by chemical denaturation as a measure of general stability. The peptide distribution of the trimers in the virtual iron(II)-assembled library was compared to that predicted from the unfolding energies of the ruthenium(II) complexes. The results were comparable, demonstrating that a virtual library approach could be extended to screen optimal packing interactions in much larger combinatorial libraries.

However, one of the limitations of this iron(II)-mediated library screen is that only the relative ratios of peptides in the trimer fraction can be observed; the actual trimers themselves cannot be observed directly. This can make resolution of a large library nearly impossible and, theoretically, would require the careful synthesis of the "winners" as heterotrimeric ruthenium(II) complexes for further structural evaluation. One way to evade this problem is to use the very powerful technique electrospray ionization (ESI) Fourier transform ion cyclotron resonance (FT-ICR) mass spectrometry.[57] This is a very high-resolution technique that results in great mass accuracy, as well as being a gentle ionization technique such that noncovalent complexes remain intact. With this technique, direct observation of the heterotrimeric iron(II)-assembled trimeric complexes was possible, and it shows great promise for the deconvolution of large virtual libraries.

Metal-Assembled Coiled Coils: A Robust de Novo Construct for Molecular Recognition

Most recently, we have become interested in the design of protein receptors for molecular recognition, as a first step toward designing biosensors and de novo enzymes. The $[M(bpy\text{-}peptide)_3]^{2+}$ maquette is a robust, well-folded, easily synthesized construct for molecular recognition studies, and it can be appended to any helical peptide sequence via solid-phase peptide synthesis.

Biosensors are protein devices that couple the molecular recognition element (the protein) to a molecule or surface that transduces a visual or electrical signal upon substrate binding. For example, the Imperiali group developed fluorescent biosensors for zinc based on the great sensitivity and specificity of zinc finger peptides for zinc(II).[58] A fluorophore was incorporated into the protein; it remained solvent-exposed in the absence of metal (when the protein was unstructured) but became buried in a hydrophobic cluster upon zinc binding (when the protein folded), thus altering the fluorescence signal. Nanomolar concentrations of Zn(II) could be detected, and also in the presence of competing metal ions Na^+, Mg^{2+}, and Co^{2+}. There are quite a few other examples of successful engineered biosensors.[59]

With the advent of nanotechnology, it has become possible to place an array of proteins on a metal surface and measure the changes in the electronic and mechanical properties of the metal upon substrate binding. Atomic force microscopy (AFM) is a technique used to visualize mixed solid−aqueous phase surfaces as well as to create new arrays by tip displacement of an existing monolayer on a surface. In this manner, it is theoretically possible to create multifunctional nanoscale devices with different proteins in separate well-defined areas of the surface. The molecular heights can be measured with good accuracy and compared to heights calculated from models.

We recently showed that the trimeric $[M(bpy\text{-}peptide)_3]^{2+}$ complex could serve as a useful protein in the construction of a nanoscale biosensor device. The protein $[Fe(\alpha pV_aL_dC26)_3]^{2+}$ (with D-cysteine residues at the C-terminus for gold ligation) was presented to a gold surface modified with C_{18} alkanethiol monolayer (Figure 6).[60] By effectively "scratching the surface" with the AFM tip, the C_{18} alkanethiols were displaced, and the protein self-assembled in a vertical orientation. The tip was used with reduced force to confirm that the proteins were grafted to the surface by measuring the height of the assembled protein monolayer. In a second generation of design, molecular recognition elements may be built into the protein architecture.

We have employed the $[M(bpy\text{-}peptide)_3]^{2+}$ complex in the screening of protein−peptide and protein−ligand interactions. The gp41 transmembrane subunit of the envelope glycoprotein of HIV-1 is responsible for fusion of the virus to the host cell. The trimeric coiled coil region of gp41 becomes exposed and vulnerable during the fusion process, so it is an attractive target to design antiviral

(55) Case, M. A.; McLendon, G. L. *J. Am. Chem. Soc.* **2000**, *122*, 8089−8090.
(56) (a) Huc, I.; Lehn, J.-M. *Proc. Natl. Acad. Sci. U.S.A.* **1997**, *94*, 2106−2110. (b) Lehn, J.-M. *Chem. Eur. J.* **1999**, *5*, 2455−2463.
(57) Cooper, H. J.; Case, M. A.; McLendon, G. L.; Marshall, A. G. *J. Am. Chem. Soc.* **2003**, *125*, 5331−5339.
(58) (a) Walkup, G. K.; Imperiali, B. *J. Am. Chem. Soc.* **1996**, *118*, 3053−3054. (b) Walkup, G. K.; Imperiali, B. *J. Am. Chem. Soc.* **1997**, *119*, 3443−3450.
(59) Hellinga, H. W.; Marvin, J. S. *Trends Biotech.* **1998**, *16*, 183−189.
(60) Case, M. A.; McLendon, G. L.; Hu, Y.; Vanderlick, T. K.; Scoles, G. *Nano Lett.* **2003**, *3*, 425−429.

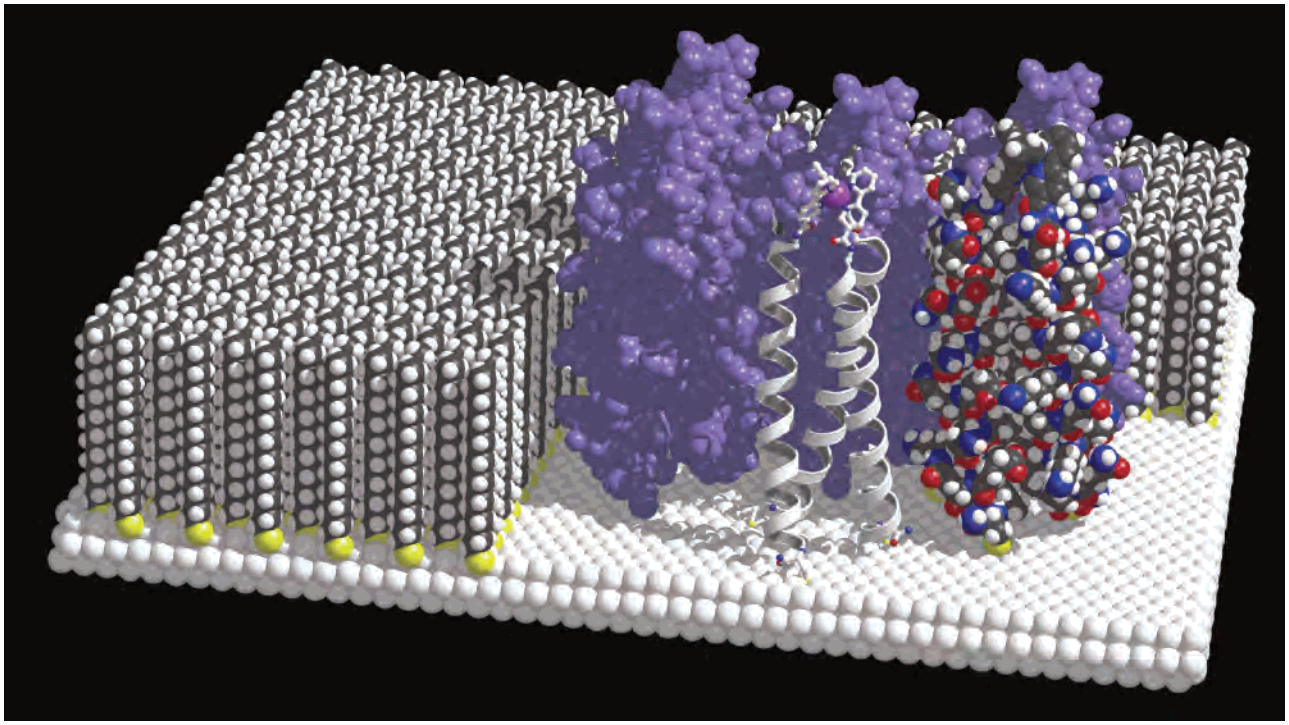

Figure 6. Model of the nanografting of the $[Fe(\alpha pV_aL_dC26)_3]^{2+}$ assembly onto a gold surface via D-cysteine residues, showing displacement of the C_{18} alkanethiol layer.[60] One protein is shown as a ribbon structure for clarity (front center), one is color-coded as a space-filling model (front right), the others are shown as van der Waals surfaces.

inhibitors to prevent fusion and subsequent infection. One of the major problems in studying this protein system is that the coiled coil domain of gp41 is not stable when isolated from the full-length gp41. However, by appending the $[M(bpy\text{-}peptide)_3]^{2+}$ maquette, this domain was stabilized and used to construct a biosensor.[61]

Two known peptide inhibitors of gp41 were synthesized, and a fluorescent dansyl group was appended to the C-termini of these peptides. When this dansyl group comes within 30 Å of an $[Fe(bpy)_3]^{2+}$ center, the fluorescence is quenched by FRET (fluorescent resonance energy transfer). The fluorescence of each peptide inhibitor was quenched in the presence of the $[Fe(bpy)_3]^{2+}$ modified gp41, thus providing evidence for a binding interaction. This biosensor system could be extended to create a competitive inhibition assay for high throughput screening of a series of peptidomimetic molecules, where the intensity of the fluorescent dansyl signal could be calibrated for binding affinity and strength.

The 33-residue GCN4-p1 peptide of the yeast transcription factor GCN4 forms dimeric coiled coils due to the interhelical hydrogen bonding of two buried asparagine residues. Alber and co-workers discovered that when this asparagine was substituted with alanine, a small cavity formed that was able to bind benzene or cyclohexane causing a switch in the oligomeric state from a dimer to a trimer.[62] However, in the absence of a strong binding ligand the system continued to form a dimer, so weak binders could not be evaluated. Furthermore, the determination of binding constants of exogenous ligands was complicated by the association of the three monomeric peptides. Templating the peptides on the $[M(bpy)_3]^{2+}$ construct allowed for a much simpler determination of binding constants without accounting for multiple equilibria.[63]

^{19}F NMR[64] titration and diffusion experiments were used to determine the binding constant of hexafluorobenzene with the metal-assembled alanine cavity trimer, $[Fe(bpyGCN4\text{-}N16A)_3]^{2+}$.[63] The fluorine nucleus is much more sensitive to changes in environment than a proton, so significant chemical shift changes occurred upon hexafluorobenzene-$[Fe(bpyGCN4\text{-}N16A)_3]^{2+}$ binding (Figure 7). Additionally, ^{19}F spectra are simple to interpret due to a lack of spectral overlap with the protein. A ^{19}F NMR competitive inhibition assay was developed to measure the binding constants of a variety of ligands by monitoring the competitive displacement of the bound hexafluorobenzene from the protein by its resulting chemical shift change. As expected, it was found that all nonpolar ligands bound more tightly in the cavity than ligands with polar groups. With this method, any ligand, no matter the solubility in water, could be tested for binding. The control protein $[Fe(bpyGCN4\text{-}N16V)_3]^{2+}$ contained no cavity and was not expected to show a binding interaction with hexafluorobenzene. There indeed was little spectral change upon addition of hexafluorobenzene (Figure 7).

(61) Gochin, M.; Kiplin G., R.; Case, M. A. *Angew. Chem., Int. Ed.* **2003**, *42*, 5325−5328.
(62) Gonzalez, L., Jr.; Plecs, J. J.; Alber, T. *Nat. Struct. Biol.* **1996**, *3*, 510−515.
(63) Doerr, A. J.; Case, M. A.; Pelczer, I.; McLendon, G. L. *J. Am. Chem. Soc.* **2004**, *126*, 4192−4198.
(64) (a) Dalvit, C.; Flocco, M.; Veronesi, M.; Stockman, B. J. *Comb. Chem. High Throughput Screening* **2002**, *5*, 605−611. (b) Dalvit, C.; Fagerness, P. E.; Hadden, D. T. A.; Sarver, R. W.; Stockman, B. J. *J. Am. Chem. Soc.* **2003**, *125*, 7696−7703.

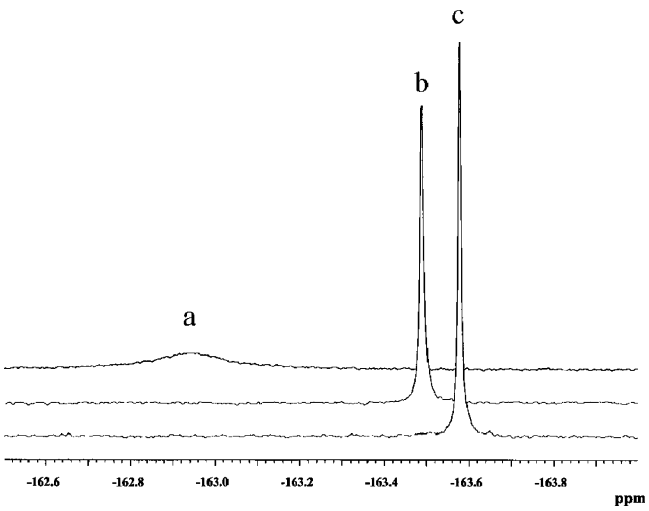

Figure 7. ^{19}F NMR spectra of saturated solutions of hexafluorobenzene in the presence of (a) $[Fe(bpyGCN4\text{-}N16A)_3]^{2+}$, (b) $[Fe(bpyGCN4\text{-}N16V)_3]^{2+}$ (control protein), and (c) buffer, exhibiting the large chemical shift change from free state (in buffer) to bound state (in presence of $[Fe(bpyGCN4\text{-}N16A)_3]^{2+}$).[63]

Table 1. Comparison of K_D's of Ligand Binding for $[Fe(bpyGCN4\text{-}N16A)_3]^{2+}$ versus $[Fe(bpyGCN4\text{-}N16G)_3]^{2+}$ by Competitive Inhibition of Hexafluorobenzene Binding[65,a]

ligand	K_D (M), $[Fe(bpyGCN4\text{-}N16A)_3]^{2+}$	K_D (M), $[Fe(bpyGCN4\text{-}N16G)_3]^{2+}$
toluene	3×10^{-6}	2×10^{-3}
p-xylene	4×10^{-6}	4×10^{-5}
cyclohexane	8×10^{-6}	2×10^{-4}
benzene	4×10^{-5}	2×10^{-3}
1,3,5-trimethylbenzene	5×10^{-5}	2.0×10^{-5}
m-xylene	1.1×10^{-4}	4×10^{-4}
hexafluorobenzene	1.1×10^{-4}	3.5×10^{-3}
tetrahydropyran	1.41×10^{-3}	7×10^{-2}
1,3,5-trioxane	1.7×10^{-3}	5×10^{0}
pyridine	4×10^{-3}	not observable
1,4-dioxane	3×10^{-2}	4×10^{-1}

[a] The ligands are arranged in order of strongest to weakest binding with the $[Fe(bpyGCN4\text{-}N16A)_3]^{2+}$ complex.

The same set of competitive inhibition experiments was performed with a glycine cavity trimer, $[Fe(bpyGCN4\text{-}N16G)_3]^{2+}$.[65] Like $[Fe(bpyGCN4\text{-}N16A)_3]^{2+}$, the glycine-modified protein also bound hydrophobic ligands more favorably than polar ligands (Table 1). However, whereas the smaller ligands such as toluene and benzene bound quite well in the alanine cavity trimer, these ligands were too small to sufficiently pack the space in the larger cavity imposed by the $[Fe(bpyGCN4\text{-}N16G)_3]^{2+}$ structure, as was indicated by weaker binding constants. Sterically larger ligands such as 1,3,5-trimethylbenzene and *p*-xylene bound most favorable in the glycine cavity trimer. Thus, a minor change in the size of the cavity (alanine to glycine) led to discriminatory binding according to size. These experiments led us to the conclusion that the cavity-containing $[Fe(bpyGCN4)_3]^{2+}$ construct was sufficiently stable and well-folded to distinguish between very similar molecules on the basis of size and packing interactions. By coupling this construct to a signaling element, sensitive biosensors might be created, with the ability to distinguish between very similar molecules.

Catalysis: The Future of Metalloprotein Design

While there are still no de novo designed enzymes that rival natural or re-engineered enzymes, progress is being made.[66] In particular, metal sites play very important roles in many designed enzymes. Simple proteins have been constructed where the metal maintains one open coordination site for receptor binding or potential catalysis.[67] Diiron sites, which can mediate oxygen binding, hydrolysis, hydroxylation, epoxidation, desaturation, and radical formation, have been designed in de novo proteins.[68] Several de novo heme-binding proteins have been designed,[69] including one that mimics photosynthesis.[70] There are quite a few examples of designed iron−sulfur proteins.[71]

Unlike inorganic or organic catalysts, protein catalysts have the potential to impart much greater substrate specificity. Designed protein cavities coupled with designed metal binding sites have the flexibility to provide great specificity and reactivity for catalytic functions unknown in nature. The $[M(bpy\text{-}peptide)_3]^{2+}$ maquette is a robust, well-folded, and well-characterized structure that has demonstrated utility in diverse applications. This construct is promising for further unique design in the future.

Acknowledgment. This work was supported by the National Science Foundation (Grant CHE-0106342) and the National Institutes of Health (GM033881 16).

IC0490573

(65) Previously unpublished data. $[Fe(bpyGCN4\text{-}N16G)_3]^{2+}$ K_D was calculated by diffusion experiments; $D_L = 6 \times 10^{-6}$ cm^2 s^{-1}, $D_{PL} = 7.7 \times 10^{-7}$ cm^2 s^{-1}, $K_D = 3.5 \times 10^{-3}$ M. For $[Fe(bpyGCN4\text{-}N16G)_3]^{2+}$ competitive inhibition experiments, $\delta_L = -163.5$ ppm, $\delta_{PL} = -163.1$ ppm. *p*-Xylene solubility in D_2O buffer was 8×10^{-4} M. See ref 63 for further experimental detail.

(66) (a) Benson, D. E.; Wisz, M. S.; Hellinga, H. W. *Curr. Opin. Biotechnol.* **1998**, *9*, 370−376. (b) Baltzer, L.; Nilsson, J. *Curr. Opin. Biotechnol.* **2001**, *12*, 355−360.

(67) (a) Merkle, D. L.; Schmidt, M. H.; Berg, J. M. *J. Am. Chem. Soc.* **1991**, *113*, 5450−5451. (b) Klemba, M.; Regan, L. *Biochemistry* **1995**, *34*, 10094−10100. (c) Corazza, A.; Vianello, F.; Zennaro, L.; Gourova, N.; Di Paolo, M. L.; Signor, L.; Marin, O.; Rigo, A.; Scarpa, M. *J. Pept. Res.* **1999**, *54*, 491−504. (d) Kiyokawa, T.; Kanaori, K.; Tajima, K.; Koike, M.; Mizuno, T.; Oku, J.-I.; Tanaka, T. *J. Pept. Res.* **2004**, *63*, 347−353.

(68) (a) Lombardi, A.; Summa, C. M.; Geremia, S.; Randaccio, L.; Pavone, V.; DeGrado, W. F. *Proc. Natl. Acad. Sci. U.S.A.* **2000**, *97*, 6298−6305. (b) Di Costanzo, L.; Wade, H.; Geremia, S.; Randaccio, L.; Pavone, V.; DeGrado, W. F.; Lombardi, A. *J. Am. Chem. Soc.* **2001**, *123*, 12749−12757. (c) Maglio, O.; Nastri, F.; Pavone, V.; Lombardi, A.; DeGrado, W. F. *Proc. Natl. Acad. Sci. U.S.A.* **2003**, *100*, 3772−3777.

(69) Kennedy, M. L.; Gibney, B. R. *Curr. Opin. Struct. Biol.* **2001**, *11*, 485−490.

(70) Cristian, L.; Piotrowiak, P.; Farid, R. S. *J. Am. Chem. Soc.* **2003**, *125*, 11814−11815.

(71) (a) Lombardi, A.; Marasco, D.; Maglio, O.; Di Costanzo, L.; Nastri, F.; Pavone, V. *Proc. Natl. Acad. Sci. U.S.A.* **2000**, *97*, 11922−11927. (b) Mulholland, S. E.; Gibney, B. R.; Rabanal, F.; Dutton, P. L. *J. Am. Chem. Soc.* **1998**, *120*, 10296−10302. (c) Gibney, B. R.; Mulholland, S. E.; Rabanal, F.; Dutton, P. L. *Proc. Natl. Acad. Sci. U.S.A.* **1996**, *93*, 15041−15046.